Non-linear mixing in coupled photonic crystal nanobeam cavities due to cross-coupling opto-mechanical mechanisms

Daniel Ramos, Ian W. Frank, Parag B. Deotare, Irfan Bulu, and Marko Lončar

Citation: Applied Physics Letters **105**, 181121 (2014); doi: 10.1063/1.4901441
View online: http://dx.doi.org/10.1063/1.4901441
View Table of Contents: http://scitation.aip.org/content/aip/journal/apl/105/18?ver=pdfcov
Published by the AIP Publishing

Non-linear mixing in coupled photonic crystal nanobeam cavities due to cross-coupling opto-mechanical mechanisms

Daniel Ramos,[a),b)] Ian W. Frank, Parag B. Deotare, Irfan Bulu, and Marko Lončar
School of Engineering and Applied Sciences, Harvard University, Cambridge, Massachusetts 02138, USA

(Received 12 September 2014; accepted 30 October 2014; published online 7 November 2014)

We investigate the coupling between mechanical and optical modes supported by coupled, freestanding, photonic crystal nanobeam cavities. We show that localized cavity modes for a given gap between the nanobeams provide weak optomechanical coupling with out-of-plane mechanical modes. However, we show that the coupling can be significantly increased, more than an order of magnitude for the symmetric mechanical mode, due to optical resonances that arise from the interaction of the localized cavity modes with standing waves formed by the reflection from thesubstrate. Finally, amplification of motion for the symmetric mode has been observed and attributed to the strong optomechanical interaction of our hybrid system. The amplitude of these self-sustained oscillations is large enough to put the system into a non-linear oscillation regime where a mixing between the mechanical modes is experimentally observed and theoretically explained. © *2014 AIP Publishing LLC*. [http://dx.doi.org/10.1063/1.4901441]

Recent developments in nanofabrication techniques allow for fabrication of mechanical resonators at nanoscale, opening the door to a plethora of novel applications in many diverse fields such as biological and mass sensing,[1–5] signal processing,[6] force measurement,[7] and quantum studies at the mesoscale.[8,9] In all of these applications involving a mechanical oscillator, the key element is the displacement transduction mechanism. Although there are different transduction approaches,[10–12] optics based techniques such as interferometry[13,14] or laser beam deflection are more attractive since they offer larger operation bandwidth, and are less sensitive to the environment surrounding the oscillator than other techniques where ionic compounds could interfere in the detection sensitivity. However, as the size of the resonator approaches the nanoscale dimensions, the optical back-action effects arises.[15] Therefore, recent years have witnessed a crescent interest in understanding the underlying physics arising from linear and nonlinear coupling of optical and mechanical degrees of freedom of nanoscale systems, besides the optomechanical actuation by means of forces originated from different mechanisms, such as scattering optical force,[16] gradient optical forces,[17] electrostrictive optical force,[18] or gyroscopic forces through optical angular momentum,[19] and their noise-control capabilities as well as their unprecedented transduction sensitivity.[20–22] In this work, we elucidate the positive impact of the optomechanical coupling on increasing the motion-transduction sensitivity, and we report the non-linear mixing arising due to the optical back-action powered self-sustained mechanical oscillations.

The system we study—coupled photonic crystal nanobeam cavities (PCNCs)—consists of two, parallel, suspended nanobeams in close proximity fabricated by electron beam lithography described elsewhere.[23] Mechanical and/or optical coupling between two such structures results in emergence of optical[23] and mechanical[24] super-modes, the situation analogous to two coupled quantum wells. The level of optical coupling, and therefore the eigen-frequencies of optical super-modes, depends on the overlap between localized optical resonances of each nanobeam. The latter can be engineered by controlling the separation between the nanobeams, the feature that has been used in the past to realize tunable/programmable photonic components.[25] At the same time, a silicon overhang in between the nanobeams, Fig. 1(a), couples out-of-plane mechanical resonances of each nanobeam, resulting in mechanical super-modes.[26]

The mechanical response of the system is studied using Finite Element Method (FEM, COMSOL Multiphysics). Each nanobeam is 20 μm long, 500 nm wide, and 220 nm thick and supports fundamental out-of-plane modes with frequency $f_0 = 4.65$ MHz and spring constant $k = 1.5$ N/m. The nanobeams are coupled via a silicon overhang of about 2 μm. This gives rise to an in-phase symmetric mode, with frequency $f_1 = 4.65$ MHz, and an out-of-phase antisymmetric mode, frequency $f_2 = 5.25$ MHz. By simply modeling the system as two coupled springs with elastic constant k_i and active mass m_i (where $i = 1,2$) that are coupled by a third massless spring (k_{12}), which represents the overhang, Fig. 1(b), the mechanical coupling constant could be calculated[24] as $\kappa = k_{12}/k$ by solving the eigenvalues equation $\mathbb{K}M^{-1}\vec{x} = \Omega^2\vec{x}$, where M is the mass matrix, Ω is the eigenvalue, $\vec{x}$ are the normalized eigenmodes of the system, and $\mathbb{K}$ is the stiffness matrix, given by $\mathbb{K} = \begin{pmatrix} 1+\kappa & -\kappa \\ -\kappa & 1+\kappa \end{pmatrix}$. This allows us to estimate the effective spring constant of the overhang to be $k_{12} = 0.19$ N/m. FEM allows to calculate the mechanical coupling constant, κ, as a function of the gap between the nanobeams. According to previous studies,[27] the coupling constant rapidly decreases with the increasing gap. We find the value of κ to be $\sim$0.13, which is similar to the values

[a)]Present address: Instituto de Microelectrónica de Madrid, IMM-CNM, CSIC, 8 Isaac Newton (PTM), Tres Cantos, 28760 Madrid, Spain.
[b)]Author to whom cprrespondence should be addressed. Electronic mail: daniel.ramos@csic.es

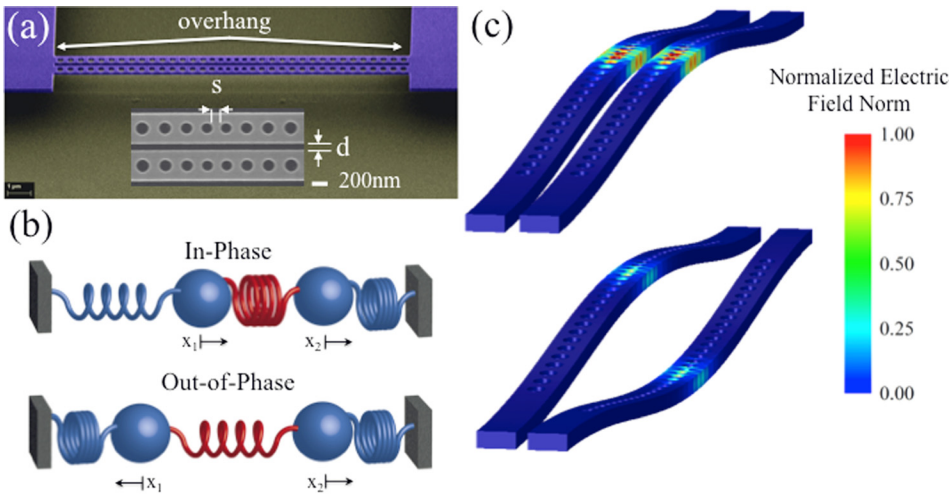

FIG. 1. (a) Scanning electron microscopy image of the experimental device. The inset shows the defect introduced to confine the electromagnetic mode. (b) Conceptual depiction of the mechanical coupling model; simulation of the mechanical coupling constant as a function of the gap separation. The symbols represent the discrete points of the calculation, whereas the line is only a guide for the eye. (c) Deformation Scale. Simulation of the mechanical symmetric and antisymmetric modes. Color Scale. Electric field norm due to the excitation of the even mode in the photonic crystal cavity.

previously reported in the literature for mechanically coupled systems.

The cavity can be viewed as a Fabry–Perot cavity with photonic crystal mirrors, which trap the nanobeam waveguide mode. To avoid the impedance mismatch between the waveguide mode and the Bloch mode, the photonic crystal mirror is tapered by reducing the hole spacing (a) and radius to match the effective indices of the evanescent mirror Bloch mode $n_{Bl} = \lambda/2a$ and the waveguide mode $n_{wg} = 2.41$. The cavities were designed using the finite-difference time-domain method being the photonic mirror pitch $a = 430$ nm, which is linearly tapered over a five hole section to $a = 330$ nm at the cavity center. The hole radius is given by $r = 0.28a$.

In addition to the mechanical coupling, two nanobeams can be coupled via optical force due to the overlap of the optical resonances of each nanobeam. In our system, symmetric optical mode is strongly dispersive, and its wavelength depends on the separation between the nanobeams, whereas the anti-symmetric optical mode is insensitive to the separation.[23] Therefore, the symmetric (even) optical mode is highly sensitive to the collective motion of the nanobeams, and even the Brownian motion of the PCNCs significantly perturbs this mode. In this work, we focus on the even optical mode, only.

Figure of merit typically used to describe the optomechanical coupling is the g_{om}, which is defined as the resonance shift of an optical mode due to a mechanical displacement.[15,28] The frequency of the resonant optical mode can be expressed in Taylor series as $\omega_O(x) = \omega_O|_{x=x_0} + (x - x_0)d\omega_O/dx|_{x=x_0} + \cdots$, where ω_0 is the optical resonance frequency, x_0 is the equilibrium position, and x is the mechanical displacement. Keeping only the first order term in the Taylor series expansion, we can write resonance frequency as $\omega_O(x) = \omega_O + (x - x_0)g_{OM}$, where we have defined the optomechanical coupling constant as $g_{OM} \equiv d\omega_O/dx|_{x=x_0}$.

Note that we can also define a universal parameter that directly relates mechanical displacement with a change in the optical resonance $L_{OM}{}^{-1} \equiv \omega_O{}^{-1} d\omega_O/dx|_{x=x_0} = \omega_O{}^{-1} g_{OM}$. L_{OM} is usually referred as the effective optomechanical coupling length, and can be analytically calculated by using perturbation theory[29] as

$$L_{OM}{}^{-1} = \frac{1}{4}\int dA\left(\vec{\psi}\cdot\hat{n}\right)\left[\Delta\varepsilon|\vec{e}_{\parallel}|^2 - \Delta(\varepsilon^{-1})|\vec{d}_{\perp}|^2\right],$$

where $\vec{\psi}$ is the displacement field, equivalent to the shape of the different mechanical modes; $\hat{n}$ is the unit vector normal to the deflected surface of the PCNCs; $\Delta\varepsilon = \varepsilon_1 - \varepsilon_2$, being ε_i, $i = 1,2$ the dielectric constant of the structure and the surrounding medium, respectively, $\Delta(\varepsilon^{-1}) = \varepsilon_1{}^{-1} - \varepsilon_2{}^{-1}$; and $\vec{d} = \varepsilon\vec{e}$.

We used FEM calculations to evaluate the optomechanical coupling length between the even optical mode and both symmetric and anti-symmetric mechanical modes, taking into account the actual mode profiles.[30] Results are shown in Fig. 1(c) where the deformed shape of the beam corresponds with the mechanical displacement field whereas the color scale represents the electric field norm. The g_{om} estimated through this perturbation theory calculation shows that the value for the antisymmetric mechanical mode is about 5 GHz/nm, whereas the g_{om} for the symmetric mode is only 1.8 GHz/nm. Both values were calculated for a gap size between the two nanobeam of 100 nm.

The fabricated devices were characterized using a resonant scattering setup.[31] In order to study the mechanical degrees of freedom of our system, the sample was placed inside a high vacuum chamber (working pressure of 10^{-6} Torr), which is sufficient to significantly reduce the effects of the viscous damping imposed by the air. Fig. 2 shows the optical and mechanical spectra for the same sample measured at high vacuum for different detuning of the excitation laser beam with respect to the cavity resonance. The characterization set up employs a tunable telecom laser focused via a 20× objective (NA = 0.5), through the view port of the vacuum chamber, and onto the sample. Light reflected from the sample was then collected by a photodetector. A spectrum analyzer at the output of the photodetector revealed mechanical resonance peaks, whereas the optical spectrum is acquired by synchronizing the laser sweep with the photodetector output. During the experimental characterization, the incident power at the output of the laser unit was fixed to 1mW. The measured quality factor for this optical mode at low output laser power (<200 μW, not shown) is of $\sim 10^5$. However, at large input powers, optical bistability can be observed, Fig. 2(a), and is attributed to thermal processes induced by two-photon absorption.[32]

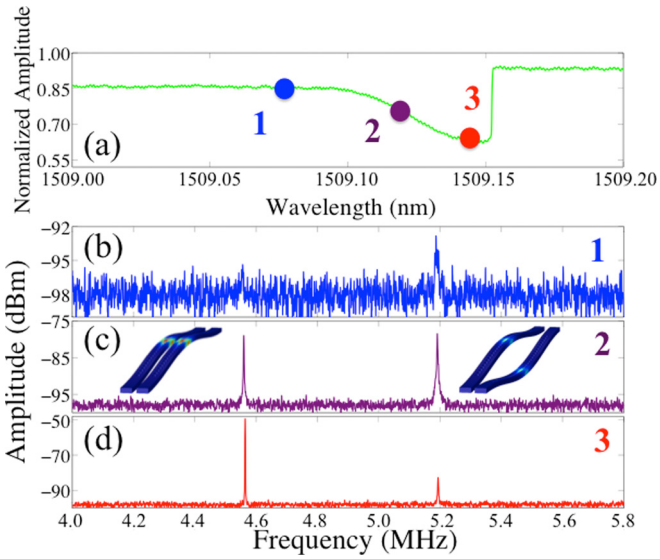

FIG. 2. Experimental measurement of the optical spectrum of the coupled photonic crystal nanobeam cavity in high vacuum (a). Experimental measurement of the mechanical spectra for different detuning. Laser wavelengths: (b) 1509.06 nm. (c) 1509.118 nm. (d) 1509.142 nm.

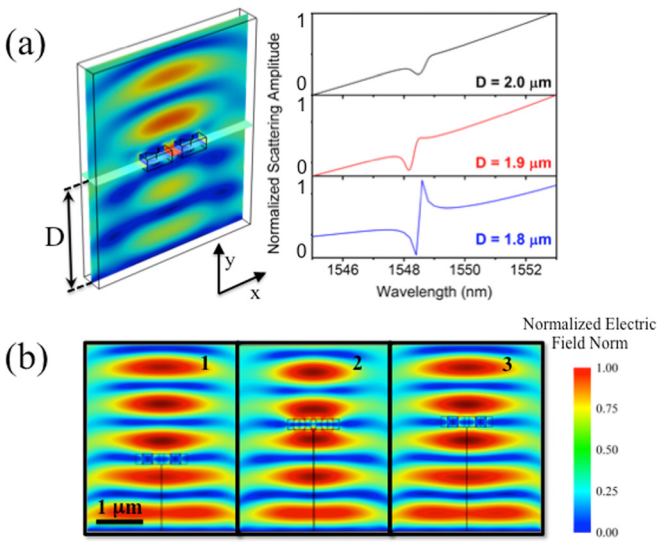

FIG. 3. (a) Slice of the three dimensional simulation of the electric field norm distribution around the photonic crystal cavity when the even optical mode is excited. Simulated optical spectra for three different distances between the nanobeams and the substrate: 2 μm, 1.9 μm, and 1.8 μm. The fano-shape is due to the interaction of the background with the resonance cavity. (b) Slices of the three dimensional simulations of a nanobeam in the photonic bandgap for different substrate distances: (1) 1550 nm, (2) 2300 nm, and (3) 2350 nm. The minima of the electric field perturbation are at the minima of the standing wave formed by the reflection of the laser on the substrate.

When the laser is completely detuned from the cavity resonance Fig. 2(b), the antisymmetric mechanical mode is barely visible, whereas the symmetric mode is completely dark. However, as the detuning from the cavity resonance is reduced, the peak corresponding to the symmetric mechanical mode arises, and at wavelength of 1509.118 nm, Fig. 2(c), is comparable to the anti-symmetric peak, while for wavelength of 1509.142 nm, Fig. 2(d) is orders of magnitude larger than the anti-symmetric peak. This is in contradiction with our estimation of optomechanical coupling based solely on localized photonic crystal nanobeam cavities resonances.

In order to understand the strong transduction of the even mode, it is important to consider an additional optomechanical coupling effect that arises from the interaction of the localized cavity modes with standing waves formed by the reflection of excitation fields from the Si substrate. Similar coupling has been previously studied in different geometries and materials,[33,34] and was found that the coupling strength can be engineered by precisely controlling the separation between the nanostructure (that supports localized modes) and the substrate (that provides broad-band reflection). In order to evaluate the coupling, FEM simulations were performed: A Gaussian beam with a waist of 3 μm, focused on the plane of the beams, was used to excite nanobeam cavities separated by a gap of 100 nm, and suspended 2 μm above the substrate. The values used here were obtained from the fabricated devices and the actual setup in order to mimic the experimental conditions. Following the previous definition of the g_{om}, we investigated the optical frequency shift as a function of the substrate distance. Color plot in Fig. 3(a) shows a slice of the tree dimensional electric field norm distribution of the double beam photonic crystal suspended over a reflective substrate at a distance D. As we can see from this simulation, the generated standing wave interacts with the photonic crystal cavity mode. As a result, the shape of the optical resonance depends on the cavity-substrate separation. In other words, coherent interaction between a background field, the standing wave, and a resonant scattering process coming from the photonic crystal cavity results in a Fano-like resonance. Due to the spatial dependence of the background field, the asymmetry in the line-shape is also modulated in the vertical coordinate, D. In Fig. 3(a), we show the simulated optical spectra for three different distances between the nanobeams and the substrate. As can be seen, when the distance is D = 2 μm, black line in Fig. 3(a)—the resonance corresponds to a lorentzian curve, however, by simply displacing the nanobeams 100 nm, red line in Fig. 3(a)—the asymmetry becomes more evident, being completely asymmetric for a distance of D = 1.8 μm, blue line in Fig. 3(a). From these simulations, we can make an estimation of the optical resonance shift as a function of the displacement from the substrate. For the symmetric mechanical mode, displacing both nanobeams in-phase, we can estimate a g_{om} of 40.1 GHz/nm, 20 times larger than the previously described coupling of localized photonic crystal cavity modes. Since the even optical mode is strongly localized in between the beams, during the antisymmetric oscillation, this optical mode is not moving at all in the surrounding electric field, and, therefore, the associated g_{om} for the antisymmetric mode is negligible (~0.5 GHz/nm). However, this mechanical mode can still be efficiently transduced by localized cavity mode only due to large deflection of nanobeams: by taking into account the equipartition theorem, we find that the amplitude of the mechanical oscillation at room temperature is ~52 pm, giving a relative displacement of the beams of about 100 pm, which results in 11 pm shift in optical resonance. This is comparable to the linewidth of our optical resonance, ~15 pm. Therefore, the Brownian motion of the antisymmetric mechanical mode is large enough to

detune the cavity resonance, thus efficiently transducing this mode as well. Therefore, we conclude that localized photonic crystal cavity mode is sufficient to efficiently transduce the antisymmetric mechanical mode, whereas the combination of localized and extended optical fields is responsible for efficient transduction of the symmetric mechanical mode.

The interaction of the nanostructure with the standing wave is described in detail in the simulations presented in Fig. 3(b). We show the spatial distribution of the electric field around the nanobeams for three different separations from the substrate, D = 1550 nm, D = 2300 nm, and D = 2350 nm. Unlike the electric field distribution in Fig. 3(a), here, we have chosen the size of the holes to place the nanobeams in the bandgap of the photonic crystal cavity. Therefore, we can see how the presence of the dielectric nanostructure perturbs the surrounding electric field, even in this case, where no resonance cavity is excited. The only place where we can put the dielectric without interaction with the background field are the minima of the standing wave, D = 1550 nm and D = 2350 nm.

It is known that when a nonlinear system is placed in a closed feedback loop, the transduction and the actuation are related, which is usually known as back action. Therefore, we expect to observe a decrease in the effective damping acting on the resonator, as the optical detuning is reduced. Furthermore, it is known[15–17,28,34–37] that in any closed feedback mechanical system, the force acting on the resonator is directly proportional to the velocity. This force is feedback in the next iteration cycle by the derivative of the new displacement (handicapped by the effective damping constant, which is smaller than the previous iteration). In a few iterations cycles, the driving force is locked to the strongest signal, ideally being a harmonic signal at the resonance frequency of the peak. Therefore, the system only amplifies the strongest signal, which corresponds to the one with the better transduction, in this case, higher g_{om}. In our geometry, this would be the symmetric mechanical mode due to the fano-like coupling explained above. Our experimental results at high output laser power (10mW) confirm this hypothesis: as shown in Fig. 4(a), symmetric mechanical mode undergoes mechanical amplifications, characterized by a decrease in the mechanical linewidth and the stiffening of the resonance,[28] whereas the linewidth of the antisymmetric mode remains unchanged. This color plot represents the oscillation amplitude as a function of mechanical frequency and laser detuning. Note that the abrupt interruption of the mechanical peaks at 1509.32 nm corresponds to the bistability region, which in this case was thermally shifted to higher wavelengths due to the larger laser power used for this experiment compared to the measurements of Fig. 2.

A mechanical resonator in the optical amplification regime experiences oscillation amplitudes larger than the usual Brownian motion, in a similar way than a forced harmonic oscillator. In this scenario, the displacement induces a stress larger than the intrinsic one, yielding to a nonlinear behavior. The Duffing model in which the resonance frequency has a quadratic dependence on the displacement accounts for the nonlinearity. Thus, the cubic term in the nonlinear equation of motion is responsible for the mixing of

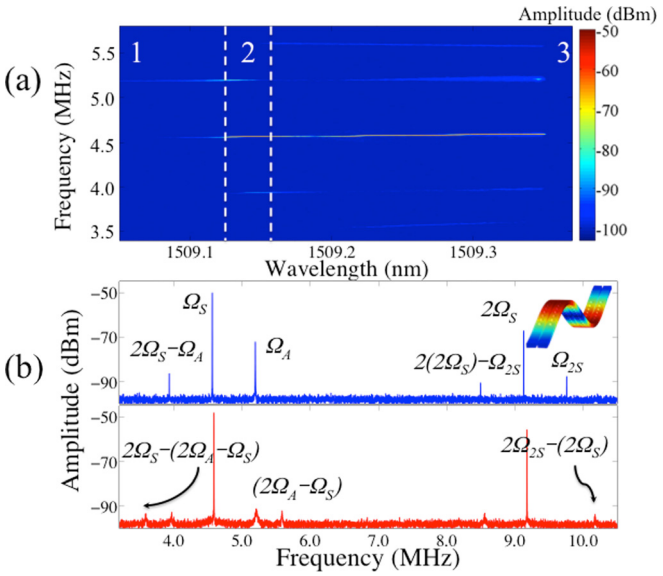

FIG. 4. Nonlinear optomechanical mixing. (a) Experimental measurement of the mechanical spectra as a function of the laser detuning. As the laser detuning is decreasing, the number of peaks in the mechanical spectra increases. The first one is the antisymmetric mode, the second the symmetric mode, region 1. Then, these two modes are mixed into different peaks linearly, region 2, and non-linearly, region 3. (b) Experimental measurement of the mechanical spectrum at two different excitation wavelengths, 1509.15 nm (blue curve) and 1509.31 nm (red curve). The labels indicate the different mechanical modes: symmetric mode (Ω_S), antisymmetric mode (Ω_A), and second flexural symmetric mode (Ω_{2S}).

the symmetric and antisymmetric frequencies. The equation of motion can be written as[38]

$$\ddot{\psi}_A + \gamma\dot{\psi}_A + \Omega_0{}^2\left(1 + 3\beta\psi_S{}^2\right)\psi_A = F_{th} + g\frac{\dot{\psi}_A}{\Omega_0},$$

where ψ is the mode profile, being the subscripts S and A the corresponding ones to the symmetric and antisymmetric modes, $\gamma = \Omega_0/Q$ is the mechanical damping factor, where Ω_0 is the mechanical resonance frequency and Q the mechanical quality factor; β is the nonlinearity strength; F_{th} is the Langevin thermal driving force; and g is the optomechanical feedback gain, that must be proportional to the light coupled into the cavity. The presence of the nonlinear term $\psi_S{}^2$ implies that the system oscillates at a frequency of $2\Omega_S$, giving rise to a response at a frequency of $2\Omega_S - \Omega_A$, blue curve (laser wavelength 1509.15 nm) in Fig. 4(b). As it is shown in the figure, the first two peaks in the spectrum are the symmetric and the antisymmetric ones, region labeled as 1 in Fig. 4(a), however, as the detuning decreases, region 2 in Fig. 4(a) and red curve (laser wavelength 1509.31 nm) in Fig. 4(b), i.e., we couple more power inside the cavity, new peaks appear as the resulting of the frequency mixing, region 3 in the color plot in Fig. 4(a).

In conclusion, we have demonstrated that the interaction of the optical resonances associated to the light confinement in subwavelength semiconductor structures with an external optical field allows to efficiently extend optomechanics to nanoscale objects. Depending on the mechanical mode, this kind of optomechanical coupling has been proved to be more efficient than the photonic cavity mode, in the case of out-of-plane mechanical resonances studied here. This discovery

opens the door to novel cavity designs to efficiently cool selected even mechanical modes instead of odd modes with the prospect of achieving the quantum limit more quickly than with cavity optomechanics. On the other hand, this phenomenon enables the development of self-sustained oscillators in which the optical energy is converted into mechanical vibration at the natural frequency. In this optical amplification regime, a nonlinear frequency mixing of the symmetric and antisymmetric mechanical modes is reported and explained in terms of the cubic term in the Duffing model.

Devices were fabricated in the Center for Nanoscale Systems (CNS) at Harvard. D.R. acknowledges financial support from the EU Grant Marie Curie IOF-2009-254996. This work was supported in part by NSF CAREER award.

[1]T. Braun, M. Ghatkesar, N. Backmann, W. Grange, P. Boulanger, L. Letellier, H. Lang, A. Bietsch, C. Gerber, and M. Hegner, Nat. Nanotechnol. **4**, 179 (2009).
[2]J. Mertens, C. Rogero, M. Calleja, D. Ramos, C. Briones, J. A. Martín-Gago, and J. Tamayo, Nat. Nanotechnol. **3**, 301 (2008).
[3]T. Burg, M. Godin, S. Knudsen, W. Shen, G. Carlson, J. Foster, K. Babcock, and S. Manalis, Nature (London) **446**, 1066 (2007).
[4]B. Lassagne, D. Garcia-Sanchez, A. Aguasca, and A. Bachtold, Nano Lett. **8**(11), 3735 (2008).
[5]E. Gil-Santos, D. Ramos, J. Martinez, M. Fernández-Regúlez, R. García, A. San Paulo, M. Calleja, and J. Tamayo, Nat. Nanotechnol. **5**, 641 (2010).
[6]B. S. Song, T. Asano, Y. Akahane, Y. Tanaka, and S. Noda, J. Lightwave Technol. **23**, 1449 (2005).
[7]D. Rugar, R. Budakian, H. J. Mamin, and B. W. Chui, Nature (London) **430**, 329 (2004).
[8]A. D. O'Connell, M. Hofheinz, M. Ansmann, R. C. Bialczak, M. Lenander, E. Lucero, M. Neeley, D. Sank, H. Wang, M. Weides, J. Wenner, J. M. Martinis, and A. N. Cleland, Nature (London) **464**, 697 (2010).
[9]J. Chan, T. P. Mayer Alegre, A. H. Safavi-Naeini, J. T. Hill, A. Krause, S. Gröblacher, M. Aspelmeyer, and O. Painter, Nature (London) **478**, 89 (2011).
[10]R. B. Karabalin, S. C. Masmanidis, and M. L. Roukes, Appl. Phys. Lett. **97**, 183101 (2010).
[11]J. Arcamone, M. Sansa, J. Verd, A. Uranga, G. Abadal, N. Barniol, M. A. F. van den Boogaart, J. Brugger, and F. Pérez-Murano, Small **5**(2), 176 (2009).
[12]K. L. Ekinci and M. L. Roukes, Rev. Sci. Instrum. **76**, 061101 (2005).
[13]N. O. Azak, M. Y. Shagam, D. M. Karabacak, K. L. Ekinci, D. H. Kim, and D. Y. Jang, Appl. Phys. Lett. **91**, 093112 (2007).
[14]S. Babak and P. D. Ashby, Phys. Rev. Lett. **104**, 147203 (2010).
[15]T. J. Kippenberg and K. J. Vahala, Science **321**, 1172 (2008).
[16]T. Carmon, H. Rokhsari, L. Yang, T. J. Kippenberg, and K. J. Vahala, Phys. Rev. Lett. **94**, 223902 (2005).
[17]M. L. Povinelli, M. Loncar, M. Ibanescu, E. J. Smythe, S. G. Johnson, F. Capasso, and J. D. Joannopoulos, Opt. Lett. **30**(22), 3042 (2005).
[18]M. Tomes and T. Carmon, Phys. Rev. Lett. **102**(11), 113601 (2009).
[19]X. Zhang, M. Tomes, and T. Carmon, Opt. Express **19**(10), 9066 (2011).
[20]I. Favero and K. Karrai, Nat. Photonics **3**(4), 201 (2009).
[21]F. Marquardt and S. M. Girvin, Physics **2**, 40 (2009).
[22]D. Ramos, E. Gil-Santos, O. Malvar, J. M. Llorens, V. Pini, A. San Paulo, M. Calleja, and J. Tamayo, Sci. Rep. **3**, 3445 (2013).
[23]P. B. Deotare, M. W. McCutcheon, I. W. Frank, M. Khan, and M. Loncar, Appl. Phys. Lett. **95**, 031102 (2009).
[24]M. Spletzer, A. Raman, A. Q. Wu, X. Xu, and R. Reifenberg, Appl. Phys. Lett. **88**, 254102 (2006).
[25]I. W. Frank, P. B. Deotare, M. W. McCutcheon, and M. Loncar, Opt. Express **18**, 8705 (2010).
[26]E. Gil-Santos, D. Ramos, A. Jana, M. Calleja, A. Raman, and J. Tamayo, Nano Lett. **9**, 4122 (2009).
[27]E. Gil-Santos, D. Ramos, V. Pini, M. Calleja, and J. Tamayo, Appl. Phys. Lett. **98**, 123108 (2011).
[28]T. J. Kippenberg and K. J. Vahala, Opt. Express **15**, 17172 (2007).
[29]S. G. Johnson, M. Ibanescu, M. A. Skorobogatiy, O. Weisberg, J. D. Joannopoulos, and Y. Fink, Phys. Rev. E **65**, 066611 (2002).
[30]M. Eichenfield, R. Camacho, J. Chan, K. J. Vahala, and O. Painter, Nature (London) **459**, 550 (2009).
[31]P. B. Deotare, M. W. McCutcheon, I. W. Frank, M. Khan, and M. Loncar, Appl. Phys. Lett. **94**, 121106 (2009).
[32]Q. Quan, P. B. Deotare, and M. Loncar, Appl. Phys. Lett. **96**, 203102 (2010).
[33]D. Ramos, E. Gil-Santos, V. Pini, J. M. Llorens, M. Fernández-Regúlez, A. San Paulo, M. Calleja, and J. Tamayo, Nano Lett. **12**, 932 (2012).
[34]M. J. Burek, D. Ramos, P. Patel, I. W. Frank, and M. Loncar, Appl. Phys. Lett. **103**, 131904 (2013).
[35]P. B. Deotare, I. Bulu, I. W. Frank, Q. Quan, Y. Zhang, R. Ilic, and M. Loncar, Nat. Commun. **3**, 846 (2012).
[36]J. Bechhoefer, Rev. Mod. Phys. **77**, 783 (2005).
[37]J. Tamayo, M. Calleja, D. Ramos, and J. Mertens, Phys. Rev. B **76**, 180201(R) (2007).
[38]T. Antoni, K. Makles, R. Braive, T. Briant, P.-F. Cohandon, I. Sagnes, I. Robert-Philip, and A. Heidmann, EPL **100**, 68005 (2012).